Towards high-efficient chalcopyrite photocathodes for water splitting: the use of cocatalysts beyond Pt

Arthur Corrado Salomao[a], Mileny dos Santos Araujo[a], Hugo Leandro Sousa dos Santos [a], Marina Medina [a], Lucia Helena Mascaro *[a], and Marcos Antonio Santana Andrade Junior *[a].

[a]   Mr A C Salomao, Ms M S Araujo, M.Sc. H L S dos Santos, M.Sc. M Medina, Prof L H Mascaro, Dr M A S Andrade Jr
        Department of Chemistry
        Federal University of São Carlos
        Rodovia Washington Luis, 13565-905, São Carlos, Brazil
        E-mail: lmascaro@ufscar,br
                marcos_asaj@hotmail.com

Abstract: Solar radiation is a renewable and clean energy source used in photoelectrochemical cells (PEC) to produce hydrogen gas as a powerful alternative to carbon-based fuels. Semiconductors play a vital role in this approach, absorbing the incident solar photons and converting them into electrons and holes. The hydrogen evolution reaction (HER) occurs in the interface of the p-type semiconductor that works as a photocathode in the PEC. Cu-chalcopyrite such as Cu(In, Ga)(Se,S)$_2$ (CIGS) and CuIn(Se,S)$_2$ (CIS) presents excellent semiconductor characteristics for this purpose but drawbacks as charge recombination, deficient chemical stability, and slow charge transfer kinetics, demands improvements like the use of n-type buffer layer, a protective layer, and a cocatalyst material. Concerning the last one, platinum (Pt) is the most efficient and stable material but the high price due to its scarcity imposes the search for inexpensive and abundant alternative cocatalyst. The present review highlights the use of metal alloys, transition metal chalcogenides, and inorganic carbon-based nanostructures as efficient alternative cocatalysts for HER in PEC.

1. Introduction

The high energy consumption that increases year by year and the elevated environmental pollution caused by the continuous use of fossil fuels has boosted the search for renewable, sustainable, and clean energy sources. In this context, solar energy has gained a lot of attention mainly because of its high energy capacity.[1,2] Among the benefits of solar radiation, which permits, heat generation, photovoltaic conversion, and energy chemical storage, the last is a promising and less developed approach. Currently, the photoelectrochemical cell (PEC) is the emergent technology for converting solar into chemical energy through the production of most energy-dense molecules.[3,4] In this scenario, one of the main applications of PEC is the production of hydrogen from the photoelectrochemical water electrolysis (i.e. $H_2O_{(l)} \rightarrow H_{2(g)} + \frac{1}{2} O_{2(g)}$).[5] Hydrogen is considered an attractive energy carrier because of its high energy density (122 kJ mol^{-1}) with an energy/mass ratio about 2.5 times higher than fossil fuels. Burning hydrogen generates nothing beyond water as a product, and therefore, it is considered an environmentally friendly fuel.[6,7] The semiconductors play an important role in PEC devices, they are responsible for absorbing the incident solar photons and converting them into electrons and holes.[8] In a p-type

semiconductor, the electrons photogenerated migrate to the semiconductor/electrolyte interface becoming available for reduction reactions. [8] Thus, p-type semiconductors work as photocathodes in the PEC. In this context, the photocurrent for the water reduction reaction is determined by four main coefficients described by the following equation:[9,10]

$$j_{photo} = j_0 \times \eta_{abs} \times \eta_{sep} \times \eta_{cat} \qquad (1)$$

where j_{photo} is the photocurrent, j_0 is the theoretical maximum photocurrent, η_{abs}, η_{sep} and η_{cat} are the efficiency of photon absorption, of electron-hole separation and catalytic charge transfer, respectively.

P-type Cu-chalcopyrites such as Cu(In,Ga)(Se,S)$_2$ (CIGS) and CuIn(Se,S)$_2$ (CIS) have proven to be good materials for photoelectrochemical water reduction due to the easily tunable bandgap (1.0-2.4 eV) depending on the In/Ga and Se/S ratios,[11–13] high absorption coefficients (10^4-10^5 cm^{-1})[14,15], and a band edge alignment suitable for the hydrogen evolution reaction (HER).[16,17] However, the bare Cu-chalcopyrite as photocathode exhibits a low photocurrent (at the range of μA cm^{-2}) compared to its theoretical maximum photocurrent (j_0 > 30 mA cm^{-2} under AM 1.5 G solar spectrum).[18,19] Due to the low bandgap and high absorption coefficient, the η_{abs} must be high for both CIGS and CIS. Therefore, the low photocurrents of bare Cu-chalcopyrite are due to the poor η_{sep} and η_{cat} caused by the inefficient charge separation and slow kinetics of charge transfer to the HER.[20–23] The work required to separate the photogenerated electrons and holes in bare CIGS or CIS is related to the electric field generated by the charge redistribution at the semiconductor/electrolyte interface, which is not high enough in bare Cu-chalcopyrite, resulting in a low η_{sep}.[18]

The most efficient way to improve the charge separation in these semiconductors is by the modification of the photocathodes' surface with a thin n-type buffer layer.[20,21,25] Interfacing CIS or CIGS with an n-type buffer layer (p-n junction) results in a modulated built-in field (space charge region) at the solid-solid interface that reduces recombination, prolongs the life of the carries, and improve the onset potential for HER.[26,27] Among the various n-type semiconductor, CdS is by far the most used material as a buffer layer in CIGS or CIS photocathodes.[23,28] This fact is due to the high-quality p−n junction with a favorable alignment of the conduction bands that forming a cascade

structure, which facilitates the transport of electrons from CIGS to CdS.[28,29] In addition, CdS can be deposited as a homogeneous thin film on copper chalcopyrite photocathodes by an easy and inexpensive approach, such as the chemical bath deposition (CBD) method.[30,31] Despite the efficient charge separation with the addition of the CdS layer, these photocathodes still suffer from reduced stability in the HER reactional medium.[32] To overcome this trouble, a thin layer of a stable semiconductor, with good conductivity and a large bandgap, is usually deposited over CIGS(CIS)/CdS films. Titanium oxide (TiO$_2$) is the protective layer most used in photocathodes applied in PEC for water splitting.[32,33] In addition to inhibiting the photocorrosion of the absorbent material, TiO$_2$ has a conduction band energy slightly lower than CdS that provides a band alignment at the CIGS/CdS/TiO$_2$ interface.[23,34] This band alignment enhances the transport of photogenerated electrons to the photocathode/electrolyte interface, as seen in Figure 1.

The slow kinetics of charge transfer is an important factor in the CIGS/CdS/TiO$_2$ photoelectrochemical efficiency. For water splitting, η_{cat} depends on the amount of acceptor states at the semiconductor/electrolyte interface available for the oxi-red reactions and the charge transfer rate constant, k_c, which is controlled by both electronic coupling and the driving force.[19,34] For HER, the driving force (overpotential) can be mitigated by adding suitable nanoparticles or clusters of an efficient cocatalyst. Considering photoelectrochemical water reduction, cocatalysts play three important roles:[35]

I.	They drastically reduce the activation energy (overpotential) to initiate the HER. Thus, high current densities can be achieved at low overpotentials.

II.	They assist in the separation of the electron-hole pair at the semiconductor/electrolyte interface. The photogenerated electrons are quickly transferred to the cocatalysts where they reduce the water molecule, consequently reducing the recombination of the charge carriers in the semiconductor bulk.

III.	Cocatalysts can reduce photocorrosion or unwanted photoreduction of the semiconductor. Cocatalysts act sequestering the photogenerated electrons to reduce water, with consequent inhibition of the semiconductor photodegradation.

Platinum (Pt) and other noble metals such as ruthenium and iridium have the best efficiency and stability for HER. Not by chance, Pt has been the most widely used cocatalyst for CIGS or CIS photocathodes.[25,36] However, the high price of this metal due to its scarcity, makes it unfeasible for large-scale applications. Thus, with a view to a future sustainable application of PEC for water splitting, the search for inexpensive, abundant, and efficient cocatalysts is essential.[37] Metal alloys,[38] transition metal chalcogenides[39], and inorganic carbon-based nanostructures[11] have been demonstrated good catalyst properties for HER and they have been used as substitutes to Pt as a cocatalyst for CIGS or CIS based photocathodes. Based on these statements, this review summarizes the general aspects of non-noble metals-based cocatalyst for CIGS and CIS photocathodes applied in the photoelectrochemical water reduction such as transition metal alloys and chalcogenides, and also inorganic carbon-based nanostructures.
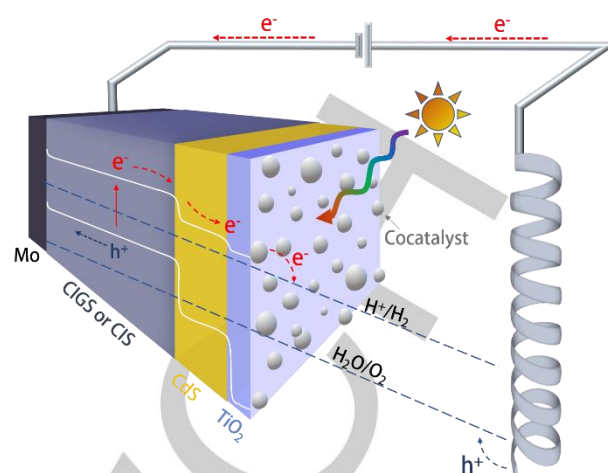
Figure 1. Schematic photoelectrochemical water splitting system using CIS or CIGS as a photocathode.

Biographical Sketch.

Arthur Corrado Salomão, currently, is a chemical engineer student and undergraduate researcher at Prof. Lucia Mascaro's group at Federal University of São Carlos (UFSCar). His research is focused on the solution-based deposition of chalcogenide thin films applied to photoelectrochemical devices for water splitting.

Mileny dos S. Araujo is currently a Chemistry undergraduate student and she is an undergraduate researcher at Prof. Lucia Mascaro´s group at the Federal University of São Carlos. Her research interest is on the deposition of ternary chalcogenide thin films for water splitting.

Hugo L. S. Santos is currently a PhD candidate at Prof. Lucia Mascaro's group at the Federal University of São Carlos. His research interests are the chemical and electrochemical synthesis of composites, metal alloys, and semiconductors, as well as the study of electrochemical and photoelectrochemical water splitting

MINIREVIEW

Marina Medina is currently a PhD candidate at Prof. Lucia Mascaro´s group at the Federal University of São Carlos. Her research interest is the electrodeposition of composites and semiconductors thin films applied as catalyst materials for electrochemical and photoelectrochemical water splitting.

Prof. Lucia H. Mascaro is currently a Professor of Physical Chemistry at the Department of Chemistry of the Federal University of Sao Carlos. She was the Coordinator of the Chemistry Graduate Program at UFSCar (2016-2018), and Chief of the Electrochemistry Division of the Brazilian Chemistry Society, SBQ (2013-2015). Her research is focused on electrochemistry and photoelectrochemistry, electrodeposition of metals and semiconductors, corrosion, electroanalytic, and water splitting.

Dr. Marcos A. S. Andrade Jr, currently, is a postdoctoral researcher at Prof. Lucia Mascaro's group at the Federal University of São Carlos. He received his PhD degree in Science from University of Campinas, Brazil, in 2016. His research interests are synthesis and characterization of semiconductors, chalcogenide thin films solar cells and chalcogenide photocathodes for water splitting.

2. Transition metal chalcogenides cocatalysts

Transition metal chalcogenides are promising candidates in many energy-related applications, including the conversion of solar energy into fuels. Because of the different possibilities of compositions with various lattice structures, morphology, tunable electronic structure, and abundance of defects sites, they may enhance the performance for water splitting.

Molybdenum disulfide (MoS_2) had its catalytic activity explored for the hydrodesulfurization process for industrial purposes[40]. However, in 2005, Hinnemann et al. [41], presented the possibility of using MoS_2 as a catalyst for the HER. In the sense to improve the catalytic activity of the crystalline and nanoparticulate form, the research evolved to the identification of the most active sites for hydrogen production. Like others two-dimensional monolayer catalysts, the basal plane of MoS_2 was proved to be inactive while the edge sites were the active catalytic part; moreover, the edge length of the crystal was directly proportional to the HER activity.[42,43] Nevertheless, economic and energy issues regarding the preparation of MoS_2 nanocrystals, such as ultra-high-vacuum and annealing at elevated temperature, hindered the catalyst´s implementation into electrocatalytic systems.[44],[45] The amorphous molybdenum sulfide (MoS_x) prepared at room

temperature and atmospheric pressure by the electrodeposition technique, exhibit remarkably high activities for HER, being more processable and scalable.[46],[47] Until then used only in electrocatalytic systems, molybdenum sulfide has received attention from other areas related to hydrogen production, being incorporated into photoelectrocatalytic systems as a cocatalyst material, replacing the high-cost Pt.

In 2015, Grätzel´s group found MoS_x as an alternative cocatalyst.[33] To increase the efficiency of the sunlight-driven water splitting, his team developed a device upon pairing the $CuIn_xGa_{1-x}Se_2$-based photocathode and a semitransparent perovskite photovoltaic device in a tandem design. The PV-PEC tandem presented a 6% solar-to-hydrogen conversion efficiency. The water splitting was investigated on bare CIGS-based photocathodes and photocathodes containing Pt or MoS_x as cocatalysts (Figure 2A). Although the overpotential for the photocathode with MoS_x was 300 mV lower than the one with Pt (Figure 2B), the photocurrent at 0 V_{RHE} was the same for both devices (~34 mA cm^{-2}, in 0.5 M H_2SO_4 under the illumination of 100 mW cm^{-2}, Table 1). Therefore, the results indicated the MoS_x electrodeposited via consecutive cyclic voltammetry as a low-cost alternative cocatalyst. [33]
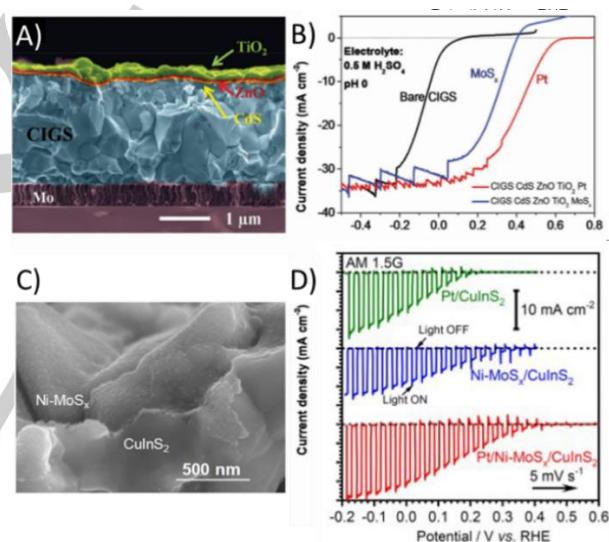
Figure 2. A) Cross-sectional view of the SEM image of TiO_2/ZnO//CIGS/CdS/Mo photocathode (Adapted with permission from Luo et al. Adv Energy Mater, 2015. [33]. Copyright 2015, by John Wiley & Sons). B) J-V curves for the bare hTiO_2/ZnO/CIGS/CdS/Mo photocathode, and the ones containing Pt and MoS_x as cocatalysts. C) SEM image of Ni-MoS_x covering $CuInS_2$ surface. D) B) J-V curves for the bare Pt/CIS/Mo and Ni-MoS_x/CIS/Mo photocathodes (Adapted with permission from Zhao et al. Sustainable Energy Fuels, 2020[48]. Copyright 2020, by Royal Society of Chemistry).

More recently, in 2020, Zhao et al.[49], in a pioneer report, demonstrated that the replacement of the well-known cocatalyst Pt in the $CuInS_2$ photocathode surface, for Ni-doped MoS_x, improved the charge separation. Firstly, the $CuInS_2$ thin film was fabricated by electrodeposition on Mo-coated soda-lime glass substrate followed by sulfurization. Ni-MoS_x was photoelectrodeposited on $CuInS_2$ (Figure 2C) by 99 scans of cyclic voltammetry, resulting in a thin layer approximately 25 nm thick. The Ni-MoS_x/$CuInS_2$ photocathode provided a photocurrent density of 9.0 mA/cm² at 0 V_{RHE} in an aqueous 0.5 M KPi electrolyte at pH 7 under AM 1.5G illumination. Comparatively,

the half-solar-to-hydrogen conversion efficiency (HC-STH) obtained for the Pt/CuInS$_2$ was 0.43% at 0.10 V$_{RHE}$ while the Ni-MoS$_x$/CuInS$_2$ reached 0.68% at 0.15 V$_{RHE}$ (Figure 2D). The onset potential value exhibited the best achievement, in which the Ni-MoS$_x$/CuInS$_2$ photoelectrode performed current at +0.4 V$_{RHE}$ while the value for the Pt/CuInS$_2$ was +0.24 V$_{RHE}$. The superior results exhibited for the Ni-MoS$_x$/CuInS$_2$ might be due to the junction formed between the CuInS$_2$ and the Ni-MoS$_x$ cocatalyst. The authors suggested that Ni-MoS$_x$ also acts as a buffer layer, resulting in the enhancement of the charge separation in the photocathode surface for hydrogen production.

Alternatively, nickel sulfide (NiS) is another low-cost and abundant chalcogenide compound use as a highly efficient cocatalyst material, specifically because of its low activation energy to form Ni-H bonds during proton reduction.[50–52] Liu and Zhou [53], loaded NiS nanoparticles on the surface of CuInS$_2$ in the photocathode CuInS$_2$/NiO/ITO. The NiS nanoparticles were synthesized via successive ionic layer adsorption and reaction (SILAR) method. The optimized quantity of NiS was reached with 15 SILAR cycles. The resulting NiS/CuInS$_2$/NiO/ITO photocathode exhibited an enhanced photocurrent of -2.23 mA/cm² at -0.6 V$_{RHE}$, representing an improvement of 175% comparing with the unpromoted CuInS$_2$ photocathode. These improved results were achieved due to the efficiency of the charge separation process by the incorporation of NiS cocatalyst.[53] Cobalt sulfide is also a low-cost, eco-friendly, and easily available noble metal-free catalyst, that has been showing promising results for water splitting.[21][54] All these pros are very meaningful to realize the large-scale implementation of this compound. Cobalt sulfide can be found as Co$_9$S$_8$, CoS, Co$_3$S$_4$, and CoS$_2$. Among these compounds, the CoS$_2$ exposes superior bifunctional catalytic performance, with lower overpotentials. [55]

The Co-S has a good chemical/electrochemical stability, suitable free energy for hydrogen adsorption, and can be processed at low temperatures. [21] In addition, the use of this material as a cocatalyst shifts anodically the onset potential of the PEC device's photocathode. Wang et al. reported a larger shift of the onset potential for chalcopyrite-based photocathodes (Co-S/ZnO/CdS/CIGS/Mo) (+0.89 V$_{RHE}$), compared to Pt (+0.85 V vs V$_{RHE}$ for Pt). It reveals an efficient transference of photo-induced carriers from CIGS to H$^+$/H$_2$ redox couples in the electrolyte.[21] Furthermore, they[21] reached, approximately, at the same conditions, a higher photocurrent density with Co-S as cocatalyst (-2.5 mA/cm² at 0.0 V vs V$_{RHE}$) compared to Pt (-1.25 mA/cm² at 0.0 V vs V$_{RHE}$).

Copper-based compounds have been also intensively used in photoelectrochemical reduction reactions since Copper (Cu) is an earth-abundant element with many oxidation states, bio-relevance, and rich coordination chemistry. [56] However, the very poor H adsorption on its active site is a bottleneck for its practical implementation, since this step is fundamental for the effectiveness of an electrocatalyst for hydrogen obtaining. [57]. Therefore, some attempts have been made over the past few years to boost the H adsorption on copper. An effective method is based on tuning the coordination environment of copper catalytic sites surrounded by different anions such as N, P, and O. Although the apparent improvement of the electrocatalytic activity, these compounds suffer from poor stability at the HER medium. On the other hand, when Cu atoms are coordinated with S, CuS has a small solubility product (Ksp) value, and it guarantees high catalyst stability.[58]

In addition, the CuS seems particularly suitable for applications in HER catalysis, because of some intrinsic properties: empty 3p-orbitals and high density of electrons and holes in its structure, which promotes electron transportation. [59] In addition, CuS can offer plenty of permeable channels for electrolyte diffusion due to its unique anisotropic structure. [60]

Kim and co-workers [61] reached a photocurrent density of approximately -11.5 mA/cm^2 and a stable photocurrent of −8 mA/cm^2 for 3h at 0 V$_{RHE}$, with a grown-in Cu$_x$S method at Cu-rich CIGSSe (Cu$_x$S/CIGSSe/Mo). Firstly, they deposited a Cu-rich Cu-In-Ga film with Cu/(In+Ga) = 1.00 ratio on Mo. After that, for the chalcogenation process of CuInGa precursor film, they separated in two steps: (i) simultaneous selenization and sulfurization using a mixture of Se vapor and H$_2$S gas elevating the temperature from 150 to 460 °C, and (ii) sulfurization using H$_2$S alone at the slightly varied temperature between 460 and 485 °C. Due to the formation temperature of Cu$_x$Se (~320 °C) being lower than that of Cu$_x$S(~360 °C), after the first step, the device resulted in a Se-rich state compared to the S content.[61] However, after the second step, it resulted in an S-rich state and the natural formation of the Cu$_x$S film since the remained Cu reacted with S at the second step. Finally, since it reached a photocurrent density comparable to devices that uses Pt, the copper sulfide showed to be a suitable environment-friendly and cocatalyst candidate.
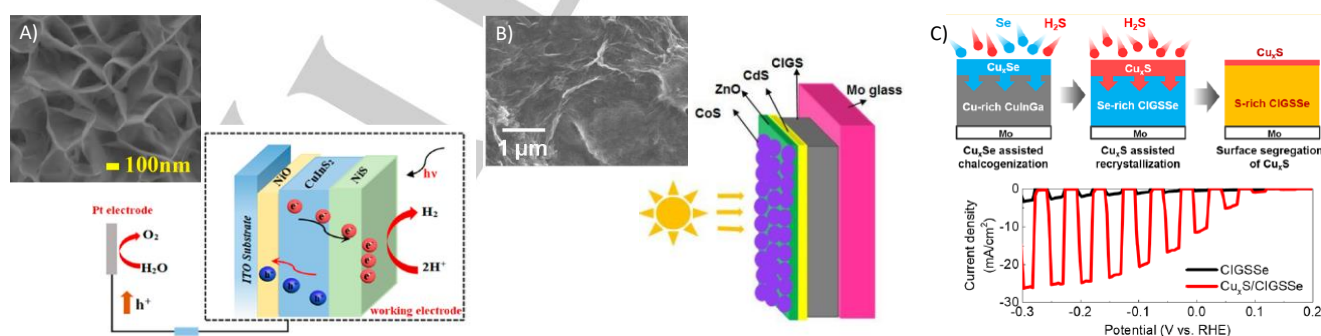
Figure 3. A) SEM image of the NiS surface deposited on cuInS$_2$/NiO/ITO photocathode and the scheme representing the PEC (Adapted with permission from Liu and Zhou et al. ACS Sustain Chem Eng, 2020 [53]. Copyright 2020, by American Chemical Society). B) SEM image of the surface and scheme of the photocathode CoS/ZnO/CdS/CIGS/Mo (Adapted with permission from Wang et al. ChemComm, 2019[21]. Copyright 2019, by Royal Society of Chemistry). C) Representation of the Cu$_x$S formation on CIGSSe films and the J-V curves of the photocathodes CIGSSe/Mo and Cu$_x$S/CIGSSe/Mo (Adapted with permission from Kim et al. ACS Energy Letters, 2019[61]. Copyright 2019, by American Chemical Society).

MINIREVIEW

However, after the second step, it resulted in an S-rich state and the natural formation of the Cu_xS film since the remained Cu reacted with S at the second step. Finally, since it reached a photocurrent density comparable to devices that uses Pt, the copper sulfide showed to be a suitable environment-friendly and cocatalyst candidate.

Transition metal chalcogenide cocatalysts are earth-abundant element-based and can be used as alternatives to Pt in chalcopyrite photocathodes. These compounds are good HER cocatalysts because they present low free energy for hydrogen absorption. In addition, the transition metal chalcogenides can form a junction with the chalcopyrite that enhances the charge separation and ensure efficient PEC hydrogen production.

3. Metal alloys

Some transition metals have good catalytic activity due to the high-density states of 4d-electrons at the Fermi level, allowing them to make strong to moderate chemisorption bonds.[62] In this context, metal alloys composed of Ni and Mo have been used for HER due to its resistance to corrosion, in acidic or basic conditions, added to its catalytic properties.[63] The interaction of Ni and Mo is beneficial, as Mo appears to stabilize Ni and make it last longer under acidic conditions.[64] Baek et al.[38] used Ni-Mo alloy as a cocatalyst in a CIGS/CdS/TiO_2 electrode configuration reaching a photocurrent of -22.5 mA cm^{-2} at pH 6.5 under 100 mW cm^{-2} of illumination. The composition of the alloy has a ratio of 4:1 Ni:Mo. As presented by Highfield et al.[65], the Ni_4Mo solution is easier to prepare and, in this case, Mo is incorporated into the Ni-centered face cubic structure. The concentration of Mo in the alloy must be controlled so that the cocatalyst can present its maximum efficiency for HER. Since Ni is a ferromagnetic material and Mo is paramagnetic, a decreased magnetization occurs when the Mo content increases, due to the Ni d orbital filling up. As reported in the literature, when the magnetization disappears, there is a decrease in the catalytic activity.[66] Still, as H is adsorbed on Ni, at the moment that the depletion of electron density at level d taking part, Ni deactivation will occur.[67] This entire process is characterized as the discharge of protons into the catalyst, known as the Volmer reaction and the first step of the Volmer-Heyrovsky reaction.[38] After H adsorption on Ni, this H falls into the so-called "trap" of Mo to complete the second stage of the Volmer-Heyrovsky reaction. This step occurs due to the disturbance of the Fermi level of Mo, which is only marginal in this case, probably because of its high character d.[65] In the Mo active site, where there is the adsorbed H, occurs the connection of a proton and an electron to the hydrogen formation in the final Heyrovsky step.[38] The synergy effect of Ni and Mo forming the alloy improves the mechanism for HER.[65] Ni-Mo was used as cocatalyst on Ni-Mo/TiO_2/CdS/CIGS/Mo photocathode (Figure 3A). Baek et al.[38], studied the effect of the electrolyte pH (0.4 to 14) on the photocurrent generated from water splitting and on the stability of the photocathode. Under acidic conditions, HER occurred more easily, with Volmer's reaction happening quickly and Heyrovsky as the slow and determining step of the reaction. This is because, at different pHs, the reaction's overpotential tends to change. A cocatalyst can enhance HER if the activation energy is reduced, which in this case is the overpotential. Thus, at pH 0.4 the overpotential was 42 mV, in contrast to the overpotential measured at pH 14, in which the HER mechanism

becomes more difficult with a higher overpotential of 53 mV. At pH 14, Volmer and Heyrovsky reactions become slower.[38]
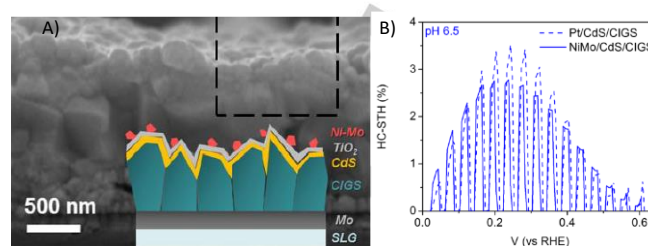

Figure 4. A) Cross-sectional view of the SEM image of Ni-Mo/TiO_2/CdS/CIGS/Mo photocathode. B) HC-STH of Ni-Mo/TiO_2/CdS/CIGS/Mo and Pt/TiO_2/CdS/CIGS/Mo photocathodes in 0.5 M Na_2SO_4 in phosphate buffer solution pH 6.5 under chopped 100 mW cm^{-2} illumination (Adapted with permission from Baek et al. CerSusChem, 2018 [38]. Copyright 2018, by John Wiley & Sons)

The authors also investigated the time effect for Ni-Mo deposition (from 2 to 5 min) on the photocurrent density.[38] The best performance was reached with the Ni-Mo photocathode prepared for 3 min, in which the thickness achieved was 70 nm. This factor is important because if the Ni-Mo layer is too thick it can block the absorption of light, and that what happened when the time of deposition of Ni-Mo is long. The onset potential remained close to -0.5 V_{RHE} under all the different analyzed pH conditions, but at pH 0.4 the photocurrent is quite stable. When the reaction was performed at pH 6.5 and 9.0, photocurrent decayed after 20 min. Therefore, at pH 14, the photocathode is not stable for more than 100 seconds.

The CIGS/CdS/Pt was also tested in other pHs, and the results of instability are similar. The photocurrent values obtained at each pH in the Ni-Mo/TiO_2/CdS/CIGS/Mo configuration was -17 mA/cm², -22 mA/cm², -12.5 mA/cm², -14 mA/cm² all in 0 V_{RHE} at pH 0.4; 6.5; 9 and 14, respectively (Table 1). This same photocathode also features an HC-STH of 2.8% at 0.24 V_{RHE} and pH 6.5, which is 20% lower than that for Pt/TiO_2/CdS/CIGS/Mo(HC-STH = 3.5%) in the same condition.[38] Although there is a slight difference in efficiency, Ni-Mo is an inexpensive alternative cocatalyst for water splitting in chalcopyrite photocathodes due to its high stability in a wide range of pH conditions, and consequently, improved durability.

4. Carbon nanostructures

Despite the interest to develop Pt-free catalysts, metal-free catalysts have also been investigated regarding environmental impact due to excessive use of metals. Carbon is among one of the most abundant elements on Earth, and carbon-based materials can be produced on a large scale with lower manufacturing costs in comparison to metal compounds. [68,69] Carbon nanotubes (CNT)[70], fullerene, and carbon-dots have been reported to act as effective catalysts for electrochemical HER, although also faces overpotential and kinetics issues. However, carbon compounds with electron-donating/accepting properties are ideal candidates for acting as cocatalysts in solar-induced reactions. Carbon nanostructures can function to promote charge separation and transfer, and enhance active sites, and accelerate the kinetics of water splitting reaction.[71]
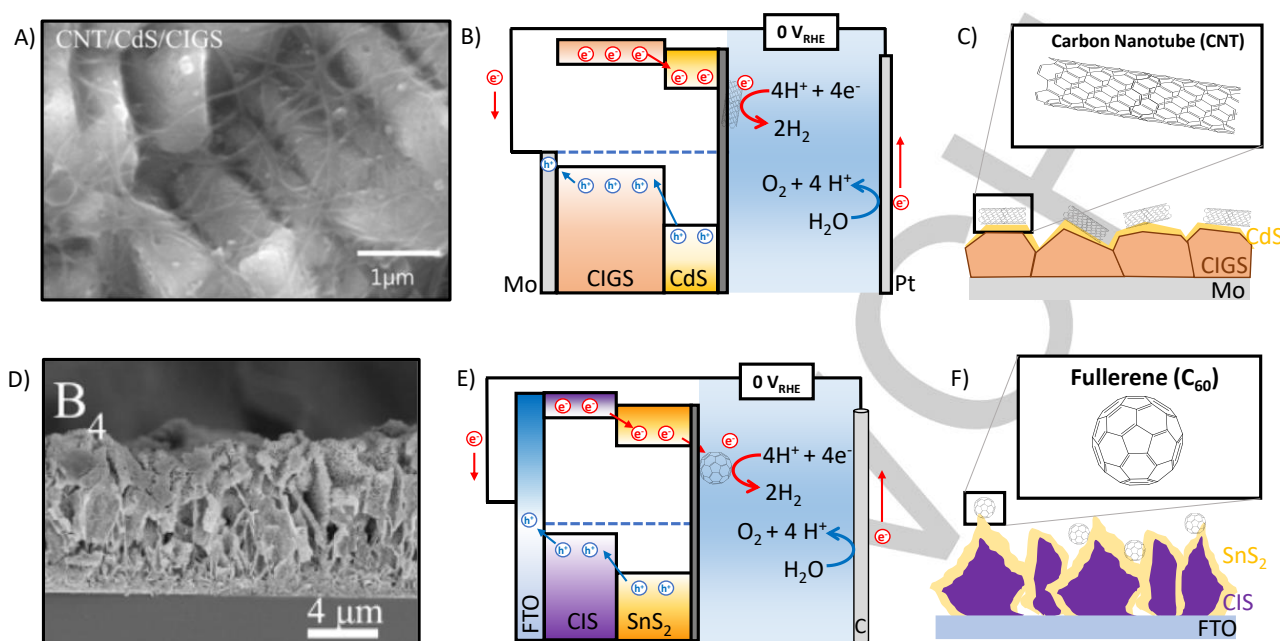
Figure 5. A) SEM image showing the carbon nanotubes covering the photocathode CdS/CIGS/Mo. B) Schematic diagram of the photoinduced charge-transfer mechanism during water splitting on CNT/CdS/CIGS/Mo. C) Cross-sectional representation of the CNT/CdS/CIGS/Mo photocathode structure. D) Cross-sectional SEM image of C_{60}/SnS$_2$/CIS/FTO photocathode. E) Schematic diagram of the photoinduced charge-transfer mechanism during water splitting on C_{60}/SnS$_2$/CIS/FTO) Representation of the C_{60}/SnS$_2$/CIS/FTO photocathode structure.

Table 1. Cocatalysts on chalcopyrite-based photocathodes for water splitting.

Photocathode	Electrolyte		J_{ph} at 0 V_{RHE} mA cm^{-2}	V_{onset} (V_{RHE})	HC-STH (%)	References
	Composition	pH				
Pt/TiO$_2$/ZnO/CdS/CIGS/Mo	0.5 M H$_2$SO$_4$	0.4	-34	0.6	6*	[33]
MoS$_x$/TiO$_2$/ZnO/CdS/CIGS/Mo			-34	0.4	--	
Pt/CIS/Mo	0.5 M KPi	7	-9.2	0.2	0.4	[72]
Ni-MoS$_x$/CIS/Mo			-9	0.4	0.7	
Pt/Ni-MoS$_x$/CIS/Mo			-15.5	0.45	1.5	
NiS/CIS/NiO/ITO	0.1 M Na$_2$SO$_4$	7.5	-0.5	0.4	--	[53]
NiS/CIS/BiOCl/FTO	0.5 M Na$_2$SO$_4$	6.5	-0.15	--	--	[73]
CoS/ZnO/CdS/CIGS/Mo	0.5 Na$_2$SO$_4$	6.5	-6	0.7	2.5	[21]
Cu$_x$S/CIGS/Mo	0.5 Na$_2$SO$_4$	6.5	-8	0.1	0.3	[61]
Pt/CdS/CIGS/Mo	0.5 M Na$_2$SO$_4$	6.5	-27		3.5	[38]
Ni-Mo/CdS/CIGS/Mo	0.5 M H$_2$SO$_4$	0.4	-18	0.5	--	
	0.5 M NaPi +0.5 M Na$_2$SO$_4$	6.5	-22.5		2.8	
	0.2 M Na$_2$HPO$_4$	9	-12.5		--	
	1 M NaOH	14	-15		--	
C$_{60}$/SnS$_2$/CIS/FTO	0.5 M Na$_2$SO$_4$	6.5	-0.5	0.15	--	[74]
CNT/CdS/CIGS/Mo	0.1 M NaOH	13	-0.9	--	--	[75]

*$HC - STH = J_{H_2} \times (E_{RHE} - E_{H+/H2})/P_{total} \times 100\%$, where J_{H_2} is the maximum photocurrent, E_{RHE} is the potential in V_{RHE}, $E_{H+/H2}$ is the standard hydrogen potential (0 V_{RHE}), and P_{total} is the total intensity of incident light (1000 W m^{-2}) under the assumption of 100% Faradaic efficiency[76].

Bae et al. [77] used CNT as cocatalysts in CdS/CIGS/Mo photocathodes. CNT layer was deposited by spray-coating CNT dispersion in isopropanol on 5 x 5 cm^2 substrates. Water splitting reactions were performed in basic conditions (1 mol L^{-1} NaOH). By adding the cocatalyst layer, photocurrent at 0 V_{RHE} increased by 56% in comparison to the one for bare CIGS/CdS photocathode (~0.5 mA cm^{-2}, Table 1). Moreover, CNT also improved stability by protecting the chalcogenide layers against photocorrosion.

Fullerene (C_{60}) has also been studied as a cocatalyst in chalcopyrite-based photocathodes. Due to its delocalized conjugated structure, it acts as an electron acceptor and eases photogenerated charge separation. In the work developed by Zhang et al.[74], C_{60} is embedded in a CIS/SnS nanosheet heterostructure film. The water reduction reaction was performed using a 0.5 mol L^{-1} Na_2SO_4 solution. By adding C_{60} as cocatalyst, at -0.45 V_{RHE}, the photocurrent was 1 mA cm^{-2} higher than the produced on bare CIS/SnS photocathodes (-3.6 mA cm^{-2}). In addition, the amount of hydrogen produced was 20 times higher due to the activity of the catalyst (127 µmol cm^{-2} at -0.45 V_{RHE} during 6 h under 100 mW cm^{-2}).

Photocathode $C_{60}/SnS_2/CIS/FTO$ exhibited the lowest work function. It indicates the electrons escape fast from the film surface improving electrons' participation in the proton reduction and hydrogen evolution. C_{60} promotes an efficient charge separation across CIS/SnS heterojunction and therefore improved PEC water reduction performance.

The carbon nanostructures present important properties, such as fast electron transfer kinetics, large area (in the case of the CNT), and photostability. Their application as cocatalysts in chalcopyrite devices still presents low photocurrent in comparison to the other aforementioned alternatives, as reported in the literature. [77] However, more investigation still needs to be done about the role of the carbon nanostructures as HER cocatalysts.

5. Summary and Perspectives

Chalcopyrite-based photocathodes containing Pt as cocatalysts are highly efficient to convert solar energy to hydrogen from water splitting due to the well-known high activity of these noble metals for the hydrogen evolution reaction. However, drawbacks such as the high cost and low availability of Pt on Earth crust make it necessary to search for alternative materials. Here, in this minireview, we have highlighted recent advances in the preparation and application of alternative cocatalysts compounds like transition metal chalcogenides, alloys, and carbon nanostructures to also obtain highly efficient and stable photocathodes for hydrogen generation.

Among the transition metal chalcogenides, MoS_x has been identified as a potential alternative. Although its lower onset potential, the CIGS-based photocathode with MoS_x cocatalyst provides the same photocurrent as the one with Pt. Modifications on MoS_x would be able to recover the onset potential, and consequently, increase the efficiency. This trend was reported for CIS-photocathodes, where Ni-doped MoS_x, provided higher onset potential and similar photocurrents for hydrogen evolution on Pt/CIS/Mo.

The highest reported onset potential for water splitting on CIGS photocathodes was achieved when using CoS as cocatalyst. The record onset potential is 0.7 V_{RHE}, however, the photocurrent was far below the one reported by the Gratzel group. The efficiency of this system was 2.5%. However, if CoS would be deposited on a high-quality CIGS film with photocurrent ~30 mA cm^{-2}, HC-STH efficiency would be up to 12 %. Based on that, it may encourage more investigations on transition metal chalcogenides as cocatalysts for chalcopyrite-based photocathodes.

CIGS photocathodes containing Ni-Mo as cocatalyst present equivalent results to devices based on Pt. Therefore, there are other alloys in potential studies to be used in HER not yet tested on chalcopyrites, but which could be promising based on their applications in electrolysis. Ni-W, Ni-Mo-Fe, and Ni-Mo-Co[78] are few examples of Ni-based alloys that have been broadly studied for HER and they can also be applied as cocatalyst in photocathodes. Recently, Santos et al.[79,80] have shown that a copper insertion in Ni-Mo and Co-Mo alloys can increase catalytic activity and reduce overpotential. The addition of Cu in Ni-Mo decreased the overpotential in almost half of the values obtained for Ni-Mo electrodes (η = -154 mV for Ni-Mo and η = -86 mV dec^{-1} Ni-Mo-Cu at -10 mA cm^{-2}). The synergy of NiMo-NiCu makes Ni-Mo-Cu alloy promising for investigation as a cocatalyst in chalcopyrite photocathodes.

Although, there are only a few studies on carbon-based cocatalysts on chalcopyrite photocathodes, carbon-based electrocatalysts with low overpotential toward HER might be investigated as cocatalyst, such as, the non-metal-doped carbon N, P, and S – doped carbon, and the metal@carbon materials, which includes Co, Fe, and Ni, embedded into carbon matrix. Furthermore, B/N, S/N, and P/N couples could enhance electron-donor property by synergetic effect between the heteroatoms[81], and they can be good candidates as cocatalysts for CIS and CIGS-based devices.

The fabrication of high-quality photocathodes is very well established. However, the deposition of those cocatalysts is a challenge to not increase the cost and time of the final photocathode. Low-cost and rapid methods of deposition must be considered when investigating different cocatalysts. Zhao et al. have shown that Ni-MoS_x provided equivalent results to Pt on CIS photocathodes. According to the author's experimental procedure, Pt deposition took 30 s while Ni-MoS_x took 2 min. Although Pt is exorbitantly more expensive than Ni-MoS_x (H_2PtCl_6 cost ~241 USD/g and $(NH_4)_2MoS_4$ is ~38 USD/g, according to Sigma-Aldrich on June 06, 2021), a rapid procedure could improve to scale up device fabrication.

Chalcopyrites photocathodes have high absorptivity, photocurrent, and high HC-STH efficiency. Optimizing this photocathode to platinum-free and with earth-abundant and non-toxic based elements can result in low cost of fabrication, and more sustainable production of hydrogen from water.

Regarding future perspectives on the design of new materials, two-dimensional (2D) compounds are being proposed as an interesting noble metal-free alternative due to the large surface-to-volume ratio and the enlargement of the availability of catalytic sites.[82] Recently, theoretical investigations based on the HER process have been used to highlight the potential application of 2D materials such as Mg_3N_2 monolayer,[83] and a new family of transition metal dichalcogenides called Janus materials, MXY (M = metal, X/Y = S, Se or Te, X ≠ Y).[84,85] These investigated compounds exhibited dynamic, structural, and thermal stability added to thermoneutrality, being promising for water splitting applications.

Acknowledgments

Keywords: chalcopyrite • water splitting • cocatalyst • alloys • photoelectrochemistry

[1] B. N. Nunes, L. F. Paula, Í. A. Costa, A. E. H. Machado, L. G. Paterno, A. O. T. Patrocinio, *Journal of Photochemistry and Photobiology C: Photochemistry Reviews* **2017**, *32*, 1–20.

[2] Y. W. Phuan, W. J. Ong, M. N. Chong, J. D. Ocon, *Journal of Photochemistry and Photobiology C: Photochemistry Reviews* **2017**, *33*, 54–82.

[3] Y. Liu, Y. X. Yu, W. De Zhang, *Electrochimica Acta* **2012**, *59*, 121–127.

[4] Y. W. Phuan, W. J. Ong, M. N. Chong, J. D. Ocon, *Journal of Photochemistry and Photobiology C: Photochemistry Reviews* **2017**, *33*, 54–82.

[5] Z. Hao, Z. Guo, M. Ruan, J. Ya, Y. Yang, X. Wu, Z. Liu, *ChemCatChem* **2021**, *13*, 271–280.

[6] I. K. Kapdan, F. Kargi, *Enzyme and Microbial Technology* **2006**, *38*, 569–582.

[7] Z. Luo, R. Miao, T. D. Huan, I. M. Mosa, A. S. Poyraz, W. Zhong, J. E. Cloud, D. A. Kriz, S. Thanneeru, J. He, Y. Zhang, R. Ramprasad, S. L. Suib, *Advanced Energy Materials* **2016**, *6*, 1600528.

[8] Z. Chen, H. N. Dinh, E. Miller, *Photoelectrochemical Water Splitting: Standards, Experimental Methods, and Protocols*, Springer, New York, **2013**.

[9] H. Dotan, K. Sivula, M. Grätzel, A. Rothschild, S. C. Warren, *Energy and Environmental Science* **2011**, *4*, 958–964.

[10] X. Zhao, J. Hu, B. Wu, A. Banerjee, S. Chakraborty, J. Feng, Z. Zhao, S. Chen, R. Ahuja, T. C. Sum, Z. Chen, *Journal of Materials Chemistry A* **2018**, *6*, 16965–16974.

[11] D. Wang, C. Wang, F. P. García de Arquer, L. Zhong, L. Qian, L. Fang, P. Liu, Y. Pang, M. Liu, M. Liu, G. Zheng, D. Sinton, E. H. Sargent, H. Yang, B. Zhang, *Journal of Materials Chemistry A* **2017**, *5*, 3167–3171.

[12] A. Chirilă, S. Buecheler, F. Pianezzi, P. Bloesch, C. Gretener, A. R. Uhl, C. Fella, L. Kranz, J. Perrenoud, S. Seyrling, R. Verma, S. Nishiwaki, Y. E. Romanyuk, G. Bilger, A. N. Tiwari, *Nature Materials* **2011**, *10*, 857–861.

[13] J. Zhao, T. Minegishi, L. Zhang, M. Zhong, G. Gunawan, M. Nakabayashi, G. Ma, T. Hisatomi, M. Katayama, S. Ikeda, N. Shibata, T. Yamada, K. Domen, *Angewandte Chemie - International Edition* **2014**, *53*, 11808–11812.

[14] Y. C. Wang, C. W. Chen, T. Y. Su, T. Y. Yang, W. W. Liu, F. Cheng, Z. M. Wang, Y. L. Chueh, *Nano Energy* **2020**, *78*, 105225.

[15] L. Li, M. Li, P. Li, *Materials Characterization* **2021**, *172*, 110900.

[16] S. Mandati, P. Misra, D. Boosagulla, N. R. Tata, S. V. Bulusu, *Industrial and Engineering Chemistry Research* **2021**, *60*, 2197–2205.

[17] L. Li, M. Li, P. Li, *Materials Characterization* **2021**, *172*, 110900.

[18] T. J. Jacobsson, V. Fjällström, M. Edoff, T. Edvinsson, *Solar Energy Materials and Solar Cells* **2015**, *134*, 185–193.

[19] T. J. Jacobsson, C. Platzer-Björkman, M. Edoff, T. Edvinsson, *International Journal of Hydrogen Energy* **2013**, *38*, 15027–15035.

[20] Z. Hu, J. Gong, Z. Ye, Y. Liu, X. Xiao, J. C. Yu, *Journal of Catalysis* **2020**, *384*, 88–95.

[21] M. Wang, Y. S. Chang, C. W. Tsao, M. J. Fang, Y. J. Hsu, K. L. Choy, *Chemical Communications* **2019**, *55*, 2465–2468.

[22] J. S. Kim, S. K. Baek, Y. B. Kim, H. W. Do, Y. H. Kwon, S. W. Cho, Y. D. Yun, J. H. Yoon, H. B. R. Lee, S. W. Kim, H. K. Cho, *Nano Energy* **2018**, *46*, 1–10.

[23] J. Zhao, T. Minegishi, L. Zhang, M. Zhong, G. Gunawan, M. Nakabayashi, G. Ma, T. Hisatomi, M. Katayama, S. Ikeda, N. Shibata, T. Yamada, K. Domen, *Angewandte Chemie - International Edition* **2014**, *53*, 11808–11812.

[24] J. S. Kim, S. K. Baek, Y. B. Kim, H. W. Do, Y. H. Kwon, S. W. Cho, Y. D. Yun, J. H. Yoon, H. B. R. Lee, S. W. Kim, H. K. Cho, *Nano Energy* **2018**, *46*, 1–10.

[25] G. Gunawan, W. Septina, S. Ikeda, T. Harada, T. Minegishi, K. Domen, M. Matsumura, *Chemical Communications* **2014**, *50*, 8941–8943.

[26] B. Koo, D. Kim, P. Boonmongkolras, S. R. Pae, S. Byun, J. Kim, J. H. Lee, D. H. Kim, S. Kim, B. T. Ahn, S. W. Nam, B. Shin, *ACS Applied Energy Materials* **2020**, *3*, 2296–2303.

[27] S. Y. Chae, S. J. Park, B. koun Min, Y. J. Hwang, O. S. Joo, *Electrochimica Acta* **2019**, *297*, 633–640.

[28] M. G. Mali, H. Yoon, B. N. Joshi, H. Park, S. S. Al-Deyab, D. C. Lim, S. J. Ahn, C. Nervi, S. S. Yoon, *ACS Applied Materials and Interfaces* **2015**, *7*, 21619–21625.

[29] J. Gu, M. Ying, Y. Zhao, *Journal of Sol-Gel Science and Technology* **2021**, *97*, 672–684.

[30] J.-H. Kim, H. Han, M. K. Kim, J. Ahn, D. K. Hwang, T. J. Shin, B. K. Min, J. A. Lim, *Scientific Reports* **2021**, *11*, 1–10.

[31] B. Koo, S. W. Nam, R. Haight, S. Kim, S. Oh, M. Cho, J. Oh, J. Y. Lee, B. T. Ahn, B. Shin, *ACS Applied Materials and Interfaces* **2017**, *9*, 5279–5287.

[32] J. Luo, Z. Li, S. Nishiwaki, M. Schreier, M. T. Mayer, P. Cendula, Y. H. Lee, K. Fu, A. Cao, M. K. Nazeeruddin, Y. E. Romanyuk, S. Buecheler, S. D. Tilley, L. H. Wong, A. N. Tiwari, M. Grätzel, *Advanced Energy Materials* **2015**, *5*, 1–8.

[33] M. Chen, Y. Liu, C. Li, A. Li, X. Chang, W. Liu, Y. Sun, T. Wang, J. Gong, *Energy and Environmental Science* **2018**, *11*, 2025–2034.

[34] R. A. Marcus, N. Sutin, *Biochimica et Biophysica Acta* **1985**, *811*, 265–322.

[35] J. Ran, J. Zhang, J. Yu, M. Jaroniec, S. Z. Qiao, *Chemical Society Reviews* **2014**, *43*, 7787–7812.

[36] W. Septina, Gunawan, S. Ikeda, T. Harada, M. Higashi, R. Abe, M. Matsumura, *Journal of Physical Chemistry C* **2015**, *119*, 8576–8583.

[37] S. Zhao, J. Huang, Y. Liu, J. Shen, H. Wang, X. Yang, Y. Zhu, C. Li, *J. Mater. Chem. A* **2017**, *5*, 4207–4214.

[38] M. Baek, M. Zafar, S. Kim, D. H. Kim, C. W. Jeon, J. Lee, K. Yong, *ChemSusChem* **2018**, *11*, 3679–3688.

[39] H. Yang, D. Zhang, H. Tian, Y. Li, X. Hu, X. Gao, Z. Liang, *ChemistrySelect* **2021**, *6*, 2878–2886.

[40] R. R. Chianelli, M. H. Siadati, M. P. De la Rosa, G. Berhault, J. P. Wilcoxon, R. Bearden, B. L. Abrams, *Catalysis Reviews - Science and Engineering* **2006**, *48*, 1–41.

[41] B. Hinnemann, P. G. Moses, J. Bonde, K. P. Jørgensen, J. H. Nielsen, S. Horch, I. Chorkendorff, J. K. Nørskov, *Journal of the American Chemical Society* **2005**, *127*, 5308–5309.

[42] T. F. Jaramillo, K. P. Jørgensen, J. Bonde, J. H. Nielsen, S. Horch, I. Chorkendorff, *Science* **2007**, *317*, 100–102.

[43] X. Yang, A. Banerjee, Z. Xu, Z. Wang, R. Ahuja, *Journal of Materials Chemistry A* **2019**, *7*, 27441–27449.

[44] J. Theerthagiri, R. A. Senthil, B. Senthilkumar, A. Reddy Polu, J. Madhavan, M. Ashokkumar, *Journal of Solid State Chemistry* **2017**, *252*, 43–71.

[45] J. Zhu, L. Hu, P. Zhao, L. Y. S. Lee, K. Y. Wong, *Chemical Reviews* **2020**, *120*, 851–918.

[46] D. Merki, S. Fierro, H. Vrubel, X. Hu, *Chemical Science* **2011**, *2*, 1262–1267.

[47] M. Medina, P. G. Corradini, **2019**, *30*, 2210–2218.

[48] J. Zhao, T. Minegishi, G. Ma, M. Zhong, T. Hisatomi, **2020**, 1–8.

[49] J. Zhao, T. Minegishi, G. Ma, M. Zhong, T. Hisatomi, **2020**, 1–8.

[50] N. Jiang, L. Bogoev, M. Popova, S. Gul, J. Yano, Y. Sun, *Journal of Materials Chemistry A* **2014**, *2*, 19407–19414.

[51] S. Esmailzadeh, T. Shahrabi, G. Barati Darband, Y. Yaghoubinezhad, *Electrochimica Acta* **2020**, *334*, 135549.

[52] C. Dai, B. Li, J. Li, B. Zhao, R. Wu, H. Ma, X. Duan, *Nano Research* **2020**, *13*, 2506–2511.

[53] Z. Liu, M. Zhou, *ACS Sustainable Chemistry and Engineering* **2020**, *8*, 512–519.

[54] Y. Sun, C. Liu, D. C. Grauer, J. Yano, J. R. Long, P. Yang, C. J. Chang, *Journal of the American Chemical Society* **2013**, *135*, 17699–17702.

[55] X. Ma, W. Zhang, Y. Deng, C. Zhong, W. Hu, X. Han, *Nanoscale* **2018**, *10*, 4816–4824.

[56] M. Fan, R. Gao, Y. C. Zou, D. Wang, N. Bai, G. D. Li, X. Zou, *Electrochimica Acta* **2016**, *215*, 366–373.

[57] M. Fan, R. Gao, Y. C. Zou, D. Wang, N. Bai, G. D. Li, X. Zou, *Electrochimica Acta* **2016**, *215*, 366–373.

[58] L. Ji, L. Zhu, J. Wang, Z. Chen, *Electrochimica Acta* **2017**, *252*, 516–522.

[59] W. Du, X. Qian, M. Xiaodong, Q. Gong, H. Cao, J. Yin, *Chemistry - A European Journal* **2007**, *13*, 3241–3247.

[60] L. Ji, L. Zhu, J. Wang, Z. Chen, *Electrochimica Acta* **2017**, *252*, 516–522.

[61] B. Kim, G. S. Park, Y. J. Hwang, D. H. Won, W. Kim, D. K. Lee, B. K. Min, *ACS Energy Letters* **2019**, *4*, 2937–2944.

[62] N. V Smith, G. K. Wertheim, S. Hufner, M. M. Traum, *Physical Review B* **1974**, *10*, 3137–3206.

[63] C. Xu, J. bo Zhou, M. Zeng, X. ling Fu, X. jiang Liu, J. ming Li, *International Journal of Hydrogen Energy* **2016**, *41*, 13341–13349.

[64] J. G. Highfield, E. Claude, K. Oguro, *Electrochimica Acta* **1999**, *44*, 2805–2814.

[65] J. G. Highfield, E. Claude, K. Oguro, *Electrochimica Acta* **1999**, *44*, 2805–2814.

[66] S. Martinez, M. Metikoš-Huković, L. Valek, *Journal of Molecular Catalysis A: Chemical* **2006**, *245*, 114–121.

[67] S. Martinez, M. Metikoš-Huković, L. Valek, *Journal of Molecular Catalysis A: Chemical* **2006**, *245*, 114–121.

[68] H. Luo, Q. Guo, P. Á. Szilágyi, A. B. Jorge, M. M. Titirici, *Trends in Chemistry* **2020**, *2*, 623–637.

[69] K. T. Alali, Jing yu, D. Moharram, Q. Liu, R. Chen, J. Zhu, R. Li, P. Liu, J. Liu, J. Wang, *Carbon* **2021**, *178*, 48–57.

[70] W. Cui, Q. Liu, N. Cheng, A. M. Asiri, X. Sun, *Chemical Communications* **2014**, *50*, 9340–9342.

[71] H. Luo, Q. Guo, P. Á. Szilágyi, A. B. Jorge, M. M. Titirici, *Trends in Chemistry* **2020**, *2*, 623–637.

[72] J. Zhao, T. Minegishi, G. Ma, M. Zhong, T. Hisatomi, M. Katayama, T. Yamada, K. Domen, *Sustainable Energy and Fuels* **2020**, *4*, 1607–1611.

[73] Y. Zhang, Y. Dong, G. Wang, P. Jiang, S. Zhao, Y. Li, X. Wu, H. Miao, J. Li, J. Lyu, Y. Wang, Y. Zhu, *Catalysis Letters* **2020**, *150*, 1337–1345.

[74] F. Zhang, Y. Chen, W. Zhou, C. Ren, H. Gao, G. Tian, *ACS Applied Materials and Interfaces* **2019**, *11*, 9093–9101.

[75] H. Bae, Y. Ko, J. Park, H. Ko, S. Ryu, J. Ha, *Jornal of the Microelectronics and Packaging Society* **2019**, *26*, 107–111.

[76] W. Yang, J. H. Kim, O. S. Hutter, L. J. Phillips, J. Tan, J. Park, H. Lee, J. D. Major, J. S. Lee, J. Moon, *Nature Communications* **2020**, *11*, DOI 10.1038/s41467-020-14704-3.

[77] H. Bae, Y. Ko, J. Park, H. Ko, S. Ryu, J. Ha, *Jornal of the Microelectronics and Packaging Society* **2019**, *26*, 107–111.

[78] C. C. L. McCrory, S. Jung, I. M. Ferrer, S. M. Chatman, J. C. Peters, T. F. Jaramillo, *Journal of the American Chemical Society* **2015**, *137*, 4347–4357.

[79] H. L. S. Santos, P. G. Corradini, M. Medina, J. A. Dias, L. H. Mascaro, *ACS Applied Materials and Interfaces* **2020**, *12*, 17492–17501.

[80] H. L. S. Santos, P. G. Corradini, M. Medina, L. H. Mascaro, *International Journal of Hydrogen Energy* **2020**, *45*, 33586–33597.

[81] W. Zhou, J. Jia, J. Lu, L. Yang, D. Hou, G. Li, S. Chen, *Nano Energy* **2016**, *28*, 29–43.

[82] Y. Li, Y. L. Li, B. Sa, R. Ahuja, *Catalysis Science and Technology* **2017**, *7*, 545–559.

[83] A. Banerjee, S. Chakraborty, R. Ahuja, *International Journal of Hydrogen Energy* **2020**, *45*, 22848–22854.

[84] X. Yang, A. Banerjee, R. Ahuja, *ChemCatChem* **2020**, *12*, 6013–6023.

[85] X. Yang, A. Banerjee, R. Ahuja, *Catalysis Science and Technology* **2019**, *9*, 4981–4989.

Entry for the Table of Contents
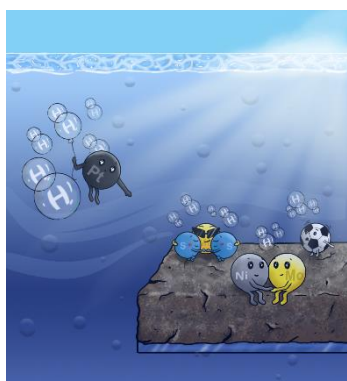
Chalcopyrite-based photocathodes containing Pt as cocatalysts are highly efficient to convert solar energy to hydrogen from water splitting. Regarding the Pt high-cost and low availability on Earth crust, here, in this minireview, we have highlighted the recent advances to replace Pt as cocatalyst and summarized the mains classes of compounds (transition metal chalcogenides, alloys, and carbon nanostructures) to also obtain highly efficient and stable photocathodes for hydrogen generation.

Institute and/or researcher Twitter usernames: @marcosasaj, @CDMF_comunica, @EnergyCine